Geophysical mapping of Mount Bonnell fault of Balcones fault zone and its implications on Trinity-Edwards Aquifer interconnection, central Texas, USA

Mustafa Saribudak[1]

Abstract

Geophysical surveys (resistivity, natural potential [self-potential], conductivity, magnetic, and ground penetrating radar) were conducted at three locations across the Mount Bonnell fault in the Balcones fault zone of central Texas. The normal fault has hundreds of meters of throw and is the primary boundary between two major aquifers in Texas, the Trinity and Edwards aquifers. In the near surface, the fault juxtaposes the Upper Glen Rose Formation on the Edwards Plateau, consisting of interbedded limestone and marly limestone, against the Edwards Group, which is mostly limestone, on the eastern down-thrown side (coastal plain). The Upper Glen Rose member is considered to be the Upper Trinity Aquifer and also a confining zone underlying the Edwards Aquifer. However, recent studies have documented a hydraulic connection between the Edwards and Upper Trinity aquifers. The uppermost portions of the Upper Trinity and the Edwards aquifers, in some places, operate as a single aquifer system, while the lowermost units of the Upper Glen Rose are confining layers between the Edwards Aquifer and the Middle Trinity Aquifer. Geophysical data, which include resistivity, natural potential, magnetic, conductivity, and ground penetrating radar, indicate not only the location of the fault but additional karstic features on the west side (Upper Glen Rose Fm.) and on the east side (Edwards Group) of the Mount Bonnell fault. Resistivity values of the Glen Rose and Edwards Group do not appear to have significant lateral variations across the fault. In other words, the Mount Bonnell fault does not appear to juxtapose different resistivity units of the Edwards Group and Upper Glen Rose member. Thus, the fault may not be a barrier for groundwater flow. With the abundant karstic features (caves, sinkholes, fractures, collapsed areas) on both sides of the fault, determined by the geophysical data, one can conclude that lateral groundwater flow (intra-aquifer) between the Edwards Aquifer and Upper Trinity is likely.

Introduction

A study of the geologic map of Austin by Garner et al. (1976) shows that normal faults along the Balcones fault zone (BFZ) are some of the main features that have shaped the geology and physiography of central Texas and its environs (Figure 1). At the regional scale, faults have positioned the geologic units (Edwards Group and underlying Glen Rose Formation) into a framework that juxtaposes contrasting rock, soil, and terrain, thereby producing a major physiographic boundary (Collins and Woodruff, 2001; Saribudak, 2011). The BFZ is a fault system consisting of numerous normal faults with hanging walls generally dropping down toward the Gulf of Mexico with displacements ranging from 98 to 853 ft (30 to 260 m) (Collins 1995; Collins, 2004). There are up to 1200 ft (365 m) of total displacement across the BFZ. Faults generally dip steeply (45–85°), varying primarily due to specific rock properties and local stress fields (Ferrill and Morris, 2008).

The BFZ includes the Edwards and Trinity aquifers, which are primary sources of water for south-central Texas communities, including the city of San Antonio. The Trinity Aquifer underlies the Edwards Aquifer through the Balcones fault zone.

The BFZ's most prominent fault is the Mount Bonnell, with a vertical throw of up to 600 ft (183 m) (Figure 1). The fault hydrogeologically juxtaposes these Cretaceous carbonate aquifers during the Miocene tectonic deformation associated with the Balcones fault zone, where the younger Edwards Group limestone has been downthrown relative to the older Glen Rose Formation (Trinity Group) (Gary et al., 2011).

The Cretaceous Edwards and Trinity aquifers of central Texas are critical groundwater resources for human and ecological needs (Gary et al., 2011). The karstic aquifers are managed separately by regional water regulatory entities, and they have been historically treated as independent systems, both scientifically and from a water-policy standpoint.

Geophysical methods have been an important component of effective hydrogeologic investigations over the Edwards Aquifer in central Texas. Geophysical surveys that employ a variety of

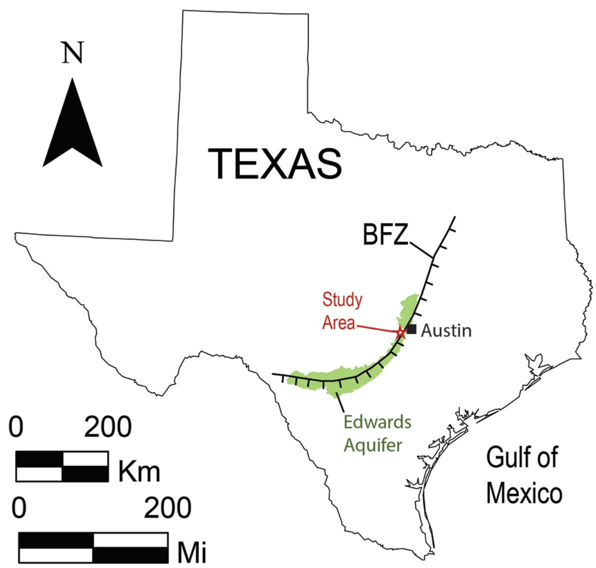

Figure 1. Texas map showing the study area of the Mount Bonnell fault and Balcones fault zone (BFZ), which is shown with a thick line. The Mount Bonnell fault trends in the northeast-southwest direction and separates the Edwards and Upper Trinity aquifers. See Figure 3 for more details on the fault and the geology.

[1]Environmental Geophysics Associates.

http://dx.doi.org/10.1190/tle35090936.1.

electrical and electromagnetic methods have been used to successfully map stratigraphy, geologic structure, and depth to the water table in major aquifer systems (e.g., Fitterman and Stewart, 1986; Connor and Sandberg, 2001). Geophysical methods are also used to delineate the locations of karst features (caves, voids, fractures, and faults) (Smith et al., 2005; Blome et al., 2008; Saribudak, 2011; Saribudak et al., 2012a; Saribudak et al., 2012b; Gary et al., 2013; Saribudak et al., 2013; Saribudak, 2015).

Multiscale geophysical surveys were conducted at two sites over the Mount Bonnell fault to determine locations of karstic features (caves, sinkhole, conduits, and faults/fractures) (Saribudak, 2011, 2012). Additional geophysical data (resistivity, natural potential, magnetic, and GPR) were acquired across a third site, Westbank Drive, in 2012 and included in this study. Furthermore, some of the geophysical data from the previous study have been reprocessed and reinterpreted. Thus, the purpose of this study is to decipher the role of the Mount Bonnell fault in the connectivity between the Edwards Aquifer and Upper Trinity Aquifer.

Hydrogeology

The karstic Edwards Aquifer is a porous, honeycombed, water-bearing rock, located within the BFZ, and is between 300 and 700 ft (91 to 213 m) thick. It includes the Edwards Group and other associated limestone, and is underlain by the Glen Rose Formation (Upper Trinity; see Figure 2), which consists of hard limestone strata alternating with marl or marly limestone.

The Upper Glen Rose member underlying the Edwards Aquifer units has historically been interpreted as a confining zone (Rose, 1972; Edwards Aquifer website: http://www.edwardsaquifer.net/geology.html). However, recent awareness of a significant connection between the Edwards and Trinity aquifers has resulted in a number of hydrogeologic investigations documenting that they actually operate as a single system in some locations and under certain circumstances (Smith and Hunt, 2010; Gary et al., 2011; Wong et al., 2014, Hunt et al., 2015). Wong et al. (2014) indicates that the uppermost 150 ft (46 m) of the Upper Glen Rose is likely part of the Edwards Aquifer, while the remainder of it is an aquitard, and portions of Upper Glen Rose are karstic. Water levels of the Upper Glen Rose are essentially the same elevation as the Edwards Aquifer (Hunt et al., 2007).

Figure 3 shows the geologic map of the Mount Bonnell fault and three locations where the geophysical surveys were conducted. The Lower Cretaceous Glen Rose Formation is at the surface to the west of the Mount Bonnell fault, while east of the fault zone the younger rocks of the Edwards Aquifer are at the surface.

Geophysical results and interpretation

Resistivity surveys were performed using AGI's SuperSting R1 and Swift system. Natural potential (self-potential) data were collected using a house-built-in NP unit. Conductivity and magnetic surveys were performed using Geonics EM31 and Geometrics G-858 instruments, respectively. GPR data were collected using GSSI SIR 2000 with a 400 MHz antenna.

Mount Bonnell fault at Bee Cave Road

Resistivity, natural potential, magnetic, conductivity, and GPR surveys were conducted across the Mount Bonnell fault at the intersection of Bee Cave Road (2244) and Camp Craft Road to the west of downtown Austin. A site map showing the approximate location of the Mount Bonnell fault and geophysical profiles is provided in Figure 4.

The resistivity and natural potential (NP) data are given in Figure 5. The resistivity data, across the fault, show resistivity values ranging between 20 and 3800 Ω.m. Low resistivity values

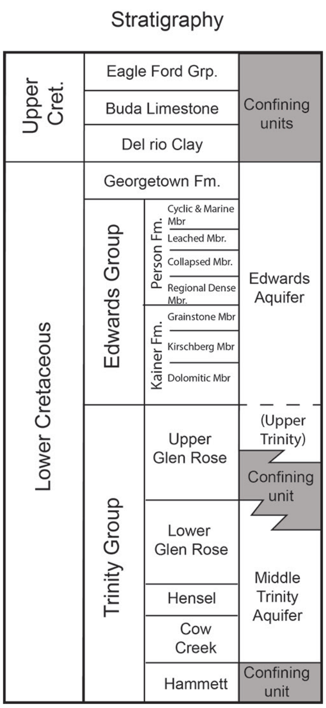

Figure 2. The stratigraphic column of the Lower and Upper Cretaceous formations within the study area illustrating hydrostratigraphic members of the Edwards and underlying Trinity Group (Small et al., 1996). Note that the Upper Glen Rose Formation is partly interpreted as an aquitard (Wong et al., 2014).

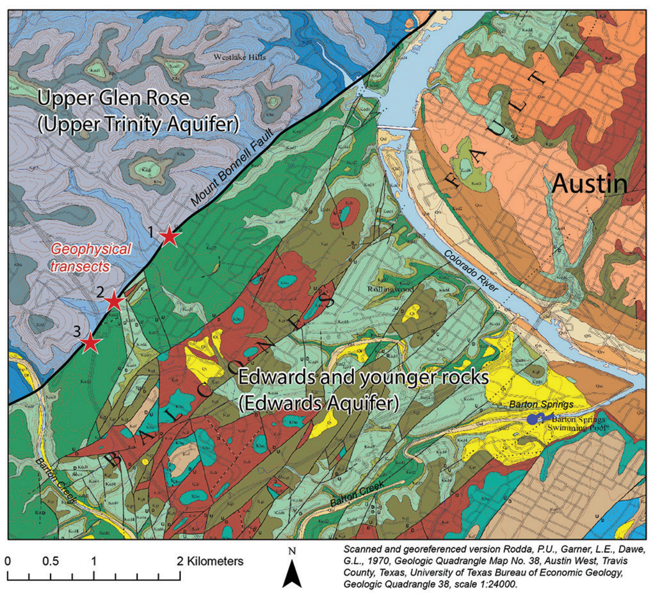

Figure 3. Geologic map indicating location of Mount Bonnell fault. Three sites were chosen to conduct geophysical surveys across the fault: (1) Bee Cave Rd; (2) Westbank Drive; and (3) Height Point Drive.

are mostly located to the south of the fault and beneath the fault location at a depth of 45 ft (14 m). There is a well-defined high-resistivity anomaly at station 251 ft (77 m), which could be due to a sinkhole. Note that an incipient sinkhole observed on the surface is close to this anomaly. The NP data shows a unique "U" type anomaly along the profile. The NP values range between 10 and -38 mV. The NP anomaly appears to be caused by a combination of the Mount Bonnell fault and the sinkhole.

The magnetic and conductivity data are displayed in Figure 6, which show high magnetic and conductivity anomalies between the stations 279 and 330 ft (85 and 100 m). It should be noted that a building wall starts where the incipient sinkhole is located and continues about 25 ft (8 m) to the southeast. Although geophysical profiles are distanced 20 ft (6 m) from the wall, both conductivity and magnetic data may be affected by the presence of the building wall. The high magnetic and conductivity anomalies correlate well with the locations of low-resistivity material (≤ 20 Ω.m). Based on this correlation, the source of the magnetic and conductivity anomalies can be attributed to magnetic soils in the subsurface (Saribudak, 2011).

The GPR data are shown in Figure 7 in two sections (A and B), which indicate a sinkhole anomaly between stations 242 and 250 ft (74 and 76 m) and a collapsed area between stations 297 and 317 ft (91 and 97 m). It should be noted that the sinkhole anomaly is located close to the observed incipient anomaly and is contained within the Glen Rose Formation. The GPR data does not indicate the location of the fault.

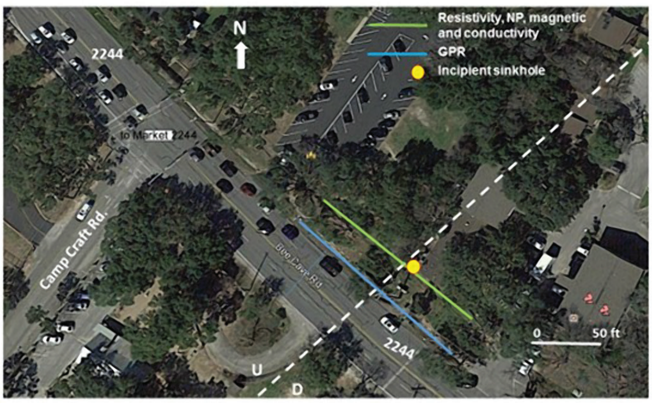

Figure 4. Site 1 map showing the location of the geophysical profiles and the Mount Bonnell fault with a white-dashed line.

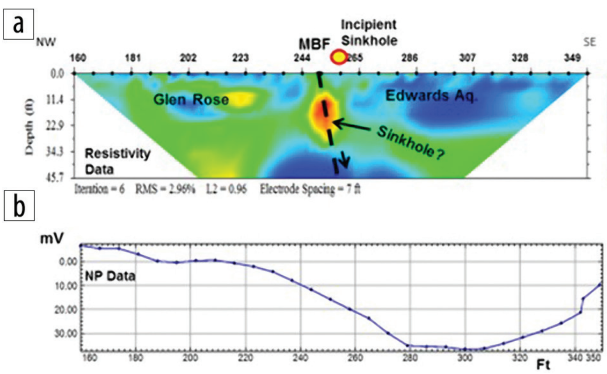

Figure 5. (a) Resistivity and (b) natural potential (NP) data along the profile. Note that there is no significant resistivity contrast across the fault. The low NP anomaly is probably due to the combination of a sinkhole and the fault itself.

Mount Bonnell fault at Westbank Drive

Magnetic, resistivity, natural potential, and GPR surveys were conducted across the Mount Bonnell fault along Westbank Drive (Figure 8).

The magnetic data (total field and vertical gradient) and NP data are shown in Figure 9. Location of the Mount Bonnell fault and known utility pipes are marked on the magnetic data for reference purposes. Steep magnetic gradients may suggest faults and fractures (Finn and Morgan, 2002) and are designated on

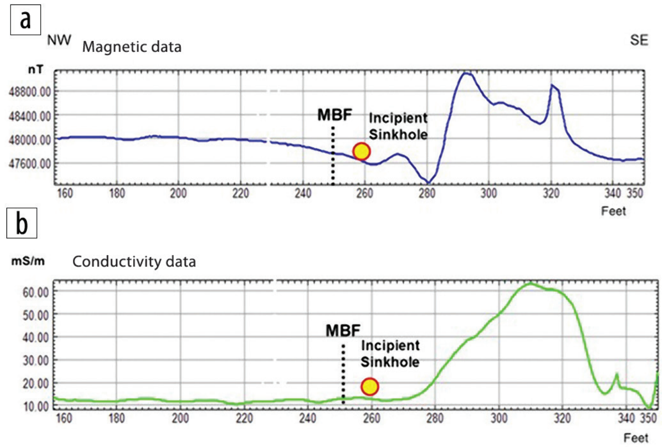

Figure 6. (a) Magnetic and (b) conductivity data indicating high magnetic and conductivity anomalies.

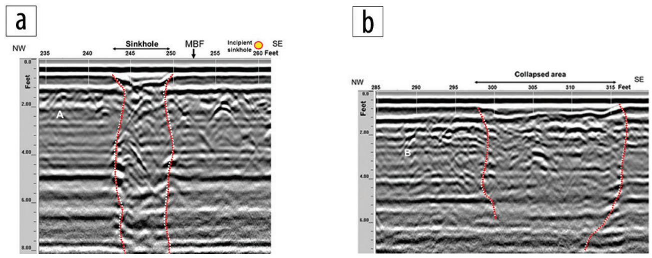

Figure 7. GPR data indicating (a) a sinkhole and (b) a collapsed area. Locations of the incipient sinkhole and Mount Bonnell fault are shown in (a).

Figure 8. Site 2 map showing the location of geophysical profiles and the Mount Bonnell fault at Westbank Drive.

the gradient data as blue stars. Note the correlation of the known location of the Mount Bonnell fault and the corresponding steep magnetic gradient at near station 700 ft (213 m). Anomalous NP locations are marked with yellow stars, and they are well correlated with the vertical gradient data, except a NP anomaly at station 100 ft (30 m).

The resistivity data were collected only along a portion of the magnetic and NP profiles. This was due to site conditions. The GPR data were collected along the entire profile, but only the GPR data with an anomalous section are shown in Figure 10, along with the resistivity data. The resistivity data indicate the resistivity distributions within the Glen Rose Formation; however, the GPR data show a "fault-like" anomaly between stations 425 and 430 ft (130 and 131 m). High-resistivity values also terminate sharply in the vicinity of the GPR anomaly, suggesting a fracture or fault.

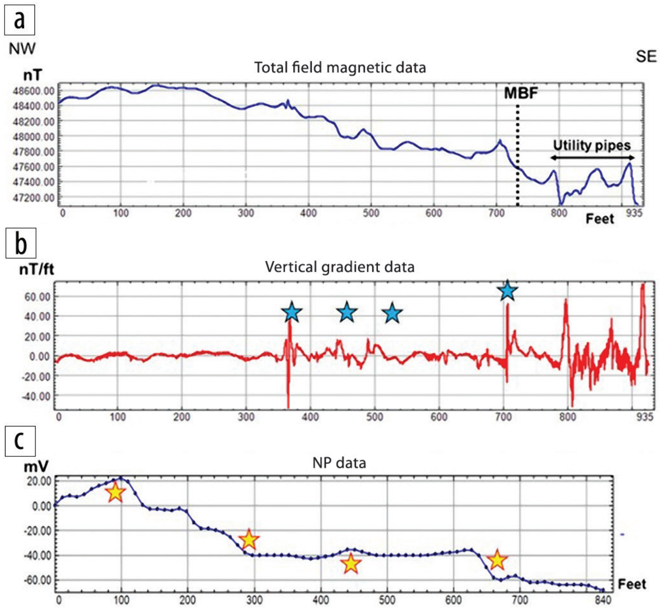

Figure 9. (a) Total earth's magnetic field, (b) vertical gradient, and (c) natural potential (NP) data across the Mount Bonnell fault. Locations of magnetic and NP anomalies are indicated with blue and yellow stars, respectively.

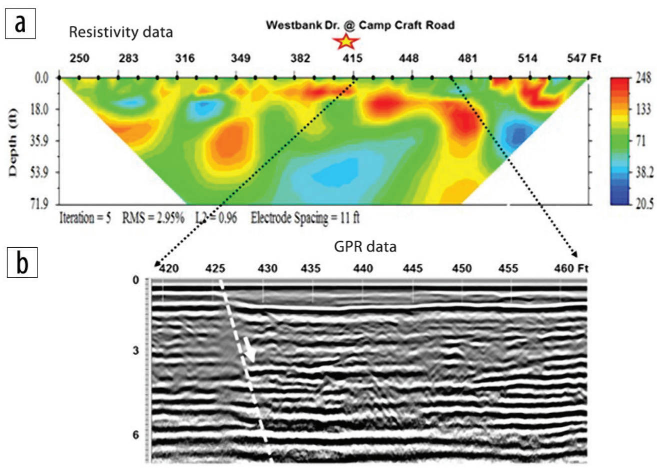

Figure 10. (a) Resistivity and (b) GPR data at Westbank site. The interpreted fault location on the GPR data coincides well with NP and magnetic anomalies (see Figure 10 for correlation).

Mount Bonnell fault at Height Drive

A site map of the study area, including the location of geophysical profiles and the Mount Bonnell fault, is shown in Figure 11. Resistivity and NP profiles were taken along a grassy ground (the light blue line), whereas the GPR survey was conducted on the asphalt (the yellow line).

Figure 12 shows the resistivity imaging and NP data along the same profile. The resistivity data indicate a very significant anomaly consisting of high- and low-resistivity anomalies between stations 280 and 320 ft (85 and 98 m). The resistivity profile does not indicate any fault anomaly where it crosses the faults; however, the NP data shows a significant anomaly (sine-wave) across the known fault location. In addition, the NP data shows an anomaly where the resistivity anomaly is observed.

The magnetic and conductivity data are shown in Figure 13. The magnetic data indicate a high anomaly, whereas the conductivity data show high and low anomalies across the resistivity anomaly. Both data sets also indicate an anomaly between stations 380 and 410 ft (116 and 125 m) where the fault is located. This anomaly is due to a known utility pipe, which is observed at the site.

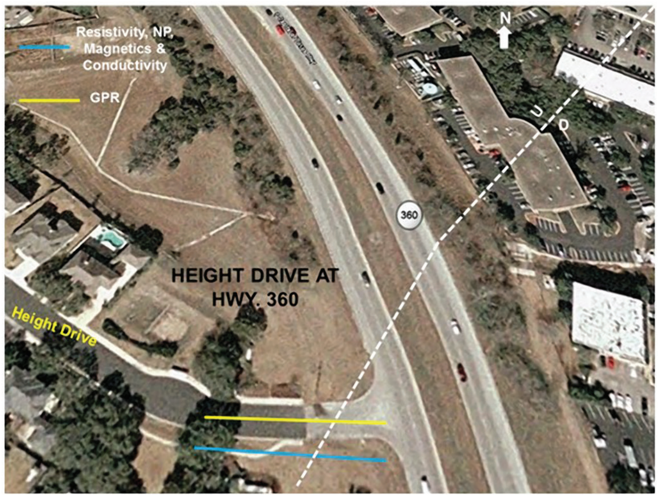

Figure 11. Site 3 map showing the locations of geophysical profile and the Mount Bonnell fault at Height Drive.

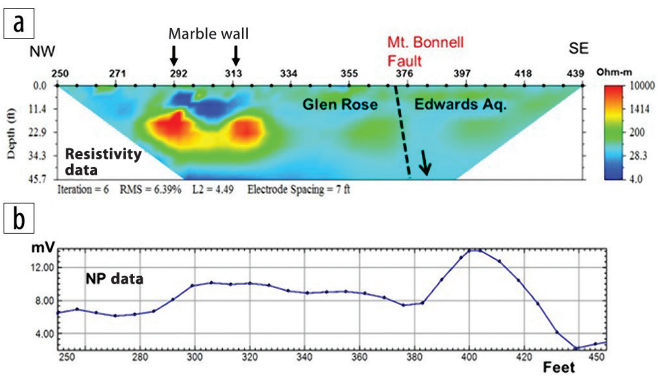

Figure 12. (a) Resistivity and (b) NP data along profile. Note the location of the Mount Bonnell fault based on the geologic map of Small et al. (1996). The resistivity data does not indicate any significant changes between juxtaposed rocks of Glen Rose and Edwards Aquifer. However, the NP data displays a significant fault-like anomaly (Reynolds, 1997).

Figure 14 provides the GPR data taken across the Mount Bonnell fault. The data show a distinct low- (Glen Rose) and high-amplitude (Edwards Aquifer) contrast across the fault, thus marking and confirming the presence of the fault.

Discussion and conclusions

All geophysical data obtained from the three locations (Bee Cave Road, Westbank Drive, and Heights Drive) across the Mount Bonnell fault indicate significant karstic anomalies. These anomalies include caves, sinkholes, collapsed areas, fractures, and faults. Locations of these anomalies are marked on a regional fault map and are shown in Figure 15.

The GPR data taken along the roads indicate significant near-surface anomalies caused by collapsing soil, sinkholes, and caves (Saribudak, 2011). These structural deformities appear to be significant enough to require continual repair as asphalt patching was noted in these areas.

In conclusion, geophysical results proved invaluable in assessing the karstic features of both Glen Rose (Upper Trinity) and Edwards Aquifer units and in locating the Mount Bonnell fault more precisely (Figure 16).

Resistivity values of the Glen Rose and Edwards aquifers do not appear to have significant lateral variations across the fault. In other words, the Mount Bonnell fault does not appear to juxtapose different resistivity units of the Edwards Aquifer and Glen Rose Formation. Thus the fault may not be a barrier for groundwater flow. With the abundant presence of karstic features (caves, sinkholes, fractures, collapsed areas) across the fault, determined by the geophysical data, one can conclude that lateral groundwater flow (intra-aquifer) between the Edwards Aquifer and Upper Trinity is very likely. TLE

Acknowledgments

I dedicate this research paper to my father, Memduh Saribudak, who passed away recently. I thank Nico Hauwert of the City of Austin for showing the Mount Bonnell fault in the field and providing the updated fault map (Figure 15). I am grateful to Brian Hunt of Barton Springs Edwards Aquifer Conservation District (BSEACD) for providing Figures 1, 2, 3, and 16. I also thank Vselovod Egorov for his help in processing the magnetic data.

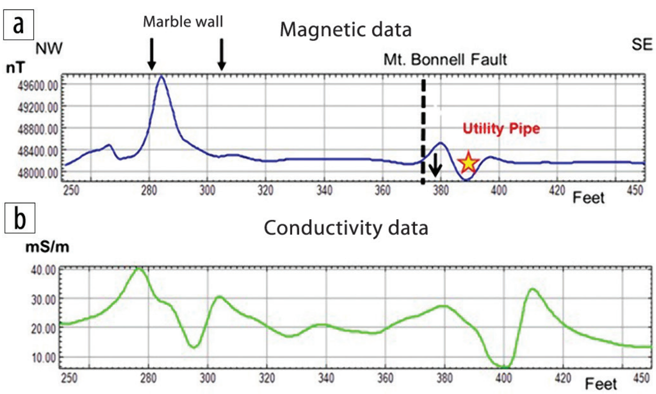

Figure 13. (a) Magnetic and (b) conductivity data across the fault. Magnetic and conductivity anomalies are observed in the northwest section of the profile. Location of the Mount Bonnell fault and a utility pipe are marked on the magnetic profile.

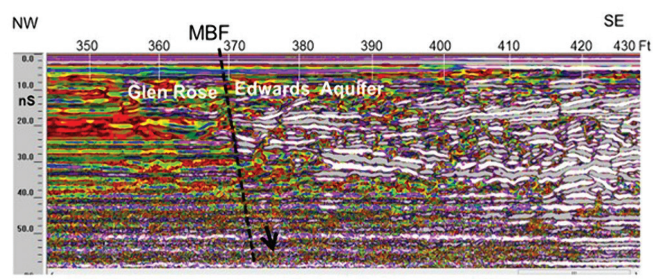

Figure 14. GPR data across the fault. The Glen Rose Formation (low amplitudes of blue, green, yellow, and brown colors) is juxtaposed to Edwards Aquifer units (high amplitudes of white and gray colors).

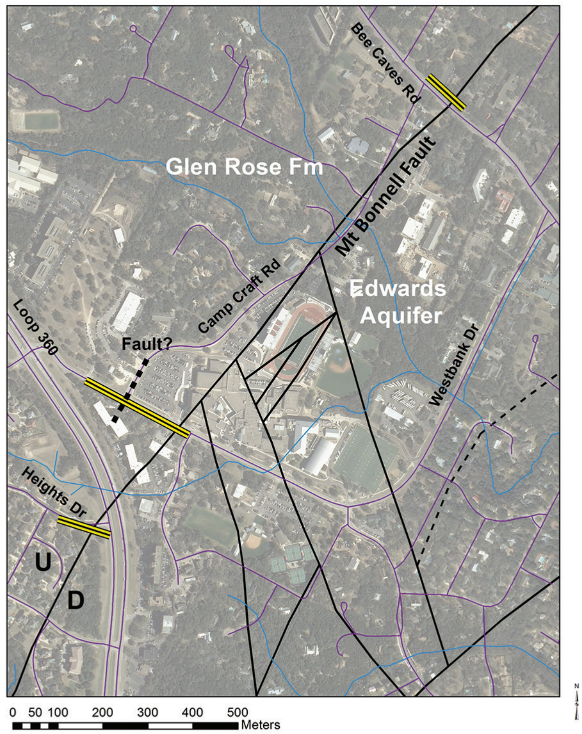

Figure 15. Site map showing locations of karstic anomalies indicated by black/yellow rectangles, across the fault. Note that karstic features are present on both sides of the fault (Small and Hauwert, 1996, and the map is modified by Hauwert in March 2016).

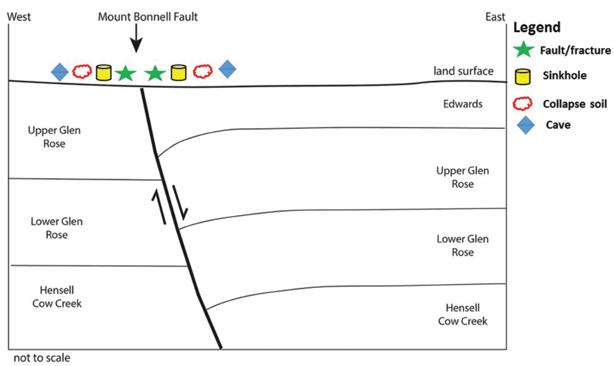

Figure 16. Schematic geologic cross-section across the Mount Bonnell fault indicating the karstic features located by the geophysical study.

Corresponding author: mbudak@pdq.net

References

Blome, C. D., B. D. Smith, D. V. Smith, J. R. Faith, A. G. Hunt, D. W. Moore, D. P. Miggins, G. B. Ozuna, and G. P. Landis, 2008, Multidisciplinary studies of the Edwards Aquifer and adjacent Trinity Aquifer of south-central Texas, Search and Discovery Article #80018, adapted from oral presentation at AAPG Annual Convention, http://pubs.usgs.gov/fs/2006/3145, accessed 4 August 2016.

Collins, E. W., 2004, Summary of the Balcones fault zone, Central Texas: A prominent zone of tertiary normal faults marking the western margin of the Texas Coastal Plain, *in* A. Hoh and B. Hunt, eds., Tectonic history of southern Laurentia: A look at Mesoproterozoic, Late-Paleozoic, and Cenozoic structures in Central Texas: Austin Geological Society Guidebook 24, 81–89.

Collins, E. W., 1995, Structural framework of the Edwards Aquifer, Balcones Fault Zone, Central Texas: Gulf Coast Association of Geological Societies Transactions, **45**, 135–142.

Collins, E.W., and C. M. Woodruff Jr., 2001, Faults in the Austin, Texas, area — Defining aspects of local structural grain, *in* C. M. Woodruff Jr. and E. W. Collins, eds., Austin Texas, and Beyond — Geology and Environment: Austin Geological Society Guidebook 21, 15–26.

Connor, C. B., and S. K. Sandberg, 2001, Application of integrated geophysical techniques to characterize the Edwards Aquifer, Texas: South Texas Geological Society Bulletin, **41**, no. 7, 11–25.

Ferrill, D. A., and A. P. Morris, 2008, Fault zone deformation controlled by carbonate mechanical stratigraphy, Balcones fault system, Texas: AAPG Bulletin, **92**, no. 3, 359–380, http://dx.doi.org/10.1306/10290707066.

Finn, A. C., and A. M. Morgan, 2002, High-resolution aeromagnetic mapping of volcanic terrain, Yellowstone National Park: Journal of Volcanology and Geothermal Research, **115**, no. 1-2, 207–231, http://dx.doi.org/10.1016/S0377-0273(01)00317-1.

Fitterman, D. V., and M. T. Stewart, 1986, Transient electromagnetic sounding for groundwater: Geophysics, **51**, no. 4, 995–1005, http://dx.doi.org/10.1190/1.1442158.

Garner, L. E., K. P. Young, P. U. Rodda, G. L. Dawe, and M. A. Rogers, 1976, Geologic map of the Austin area, Texas, *in* Garner: An aid to urban planning: The University of Texas at Austin, Bureau of Economic Geology.

Gary, M. O., B. B. Hunt, and R. H. Gary, 2011, Interconnection of the Trinity (Glen Rose) and Edwards Aquifers along the Balcones fault zone and related topics, Proceedings of the Karst Conservation Initiative; Austin, Texas, http://bseacd.org/uploads/Proceedings_Edwards_Trinity_final.pdf, accessed 4 August 2016.

Gary, M. O., D. F. Rucker, B. D. Smith, D. V. Smith, and K. Befus, 2013, Geophysical investigations of Edwards-Trinity Aquifer System at Multiple Scales: Interpreting airborne and direct-current resistivity in karst: 13th Sinkhole Conference, NCKRI Symposium 2, 195–206.

Hunt, B. B., A. S. Smith, B. J. Beery, 2007, Potentiometric maps for low to high flow conditions, Barton Springs segment of the Edwards Aquifer, central Texas: BSEACD Report of Investigations 2007-1201.

Hunt, B. B., A. B. Smith, A. Andrews, D. A. Wierman, A. S. Broun, and M. O. Gary, 2015, Relay ramp structures and their influence on groundwater flow in the Edwards and Trinity Aquifers, Hays and Travis Counties, central Texas: Presented at 14th Sinkhole Conference.

Reynolds, J. M., 1997, An introduction to applied and environmental geophysics: John Wiley & Sons.

Rose, P. R., 1972, Edwards group, surface and subsurface, Central Texas; Report of Investigations 74: Bureau of Economic Geology.

Saribudak, M., 2011, Urban geophysics: Geophysical signature of Mt. Bonnell Fault and its karstic features in Austin, Texas: Houston Geological Society Bulletin, **54**, no. 2, 49–54.

Saribudak, M., 2012, Urban geophysics: Geophysical signature of Mt. Bonnell Fault and its karstic features in Austin, Texas: Gulf Coast Associates of Geological Societies, **LXII**, 389–398.

Saribudak, M., A. Hawkins, and K. Stoker, 2012a, Do air-filled caves cause high resistivity anomalies? A six-case study from the Edwards Aquifer Recharge Zone in San Antonio, Texas: Houston Geological Society Bulletin, **54**, no. 9, 41–49.

Saribudak, M., B. Hunt, and B. Smith, 2012b, Resistivity imaging and natural potential applications to the Antioch Fault Zone in the Onion Creek/Barton Springs segment of the Edwards Aquifer: Presented at Gulf Coast Association of Geological Societies 62nd Annual Convention.

Saribudak, M., N. W. Hauwert, and A. Hawkins, 2013, Geophysical signatures of Barton Springs (Parthenia, Zenobia and Eliza) of the Edwards Aquifer, Austin, Texas, 12th Sinkhole Conference 12 proceedings, Carbonite and Evaporites, Springer.

Saribudak, M., 2015, The million dollar question: which geophysical methods locate caves best over the Edwards Aquifer? A potpourri of case studies from San Antonio and Austin, Texas, USA: Presented at 14th Sinkhole Conference, NCKRI Symposium 5, 355–364.

Small, T. A., J. A. Hanson, and N. W. Hauwert, 1996, Geologic framework and hydrogeologic characteristics of the Edwards aquifer outcrop (Barton Springs segment), northeastern Hays and southwestern Travis Counties, Texas: U.S. Geological Survey Water Resources Investigations, 96−4306, http://pubs.er.usgs.gov/publication/wri964306, accessed 4 August 2016.

Smith, B. A., and B. B. Hunt, 2010, Flow potential between stacked karst aquifers in central Texas, *in* B. Andreo, F. Carrasco, J. J. Duran, J. W. LaMoreaux, eds., Advances in research in karst media: Springer Berlin Heidelberg, 43−48, http://dx.doi.org/10.1007/978-3-642-12486-0_7.

Smith, B. D., M. J. Cain, A. K. Clark, D. W. Moore, J. R. Faith, and P. L. Hill, 2005, Helicopter electromagnetic and magnetic survey data and maps, northern Bexar County: U.S. Geological Survey Open-file Report 2005–1158.

Wong, C., J. Kromann, B. Hunt, B. Smith, and J. Banner, 2014, Investigating groundwater flow between Edwards and Trinity Aquifers in central Texas: Ground Water, **52**, no. 4, 624–639, http://dx.doi.org/10.1111/gwat.12106.